

4-24-2012

# Robust Self-Replication of Combinatorial Information via Crystal Growth and Scission

Rebecca Schulman  
*California Institute of Technology*

Bernard Yurke  
*Boise State University*

Erik Winfree  
*California Institute of Technology*

# Robust self-replication of combinatorial information via crystal growth and scission

Rebecca Schulman<sup>a,1,2</sup>, Bernard Yurke<sup>b,c</sup>, and Erik Winfree<sup>d,e,f</sup>

<sup>a</sup>Computer Science, California Institute of Technology, Pasadena, CA 91125; <sup>b</sup>Materials Science and Engineering, Boise State University, Boise, ID 83725; <sup>c</sup>Electrical and Computer Engineering, Boise State University, Boise, ID 83725; <sup>d</sup>Computer Science, California Institute of Technology, Pasadena, CA 91125; <sup>e</sup>Computation and Neural Systems, California Institute of Technology, Pasadena, CA 91125; and <sup>f</sup>Bioengineering, California Institute of Technology, Pasadena, CA 91125

Edited by Gerald F. Joyce, The Scripps Research Institute, La Jolla, CA, and approved February 21, 2012 (received for review October 31, 2011)

Understanding how a simple chemical system can accurately replicate combinatorial information, such as a sequence, is an important question for both the study of life in the universe and for the development of evolutionary molecular design techniques. During biological sequence replication, a nucleic acid polymer serves as a template for the enzyme-catalyzed assembly of a complementary sequence. Enzymes then separate the template and complement before the next round of replication. Attempts to understand how replication could occur more simply, such as without enzymes, have largely focused on developing minimal versions of this replication process. Here we describe how a different mechanism, crystal growth and scission, can accurately replicate chemical sequences without enzymes. Crystal growth propagates a sequence of bits while mechanically-induced scission creates new growth fronts. Together, these processes exponentially increase the number of crystal sequences. In the system we describe, sequences are arrangements of DNA tile monomers within ribbon-shaped crystals. 99.98% of bits are copied correctly and 78% of 4-bit sequences are correct after two generations; roughly 40 sequence copies are made per growth front per generation. In principle, this process is accurate enough for 1,000-fold replication of 4-bit sequences with 50% yield, replication of longer sequences, and Darwinian evolution. We thus demonstrate that neither enzymes nor covalent bond formation are required for robust chemical sequence replication. The form of the replicated information is also compatible with the replication and evolution of a wide class of materials with precise nanoscale geometry such as plasmonic nanostructures or heterogeneous protein assemblies.

algorithmic self-assembly | DNA nanotechnology | self-assembly

In cells, long genomes are accurately replicated via a complex replication process involving tens or sometimes hundreds of enzymes. Nearer to life's origins, a much simpler system must have been responsible for genome replication; evolution of this information then produced more and more complex forms. How a chemical system could be capable of sustained replication and evolution and yet be simple enough to arise spontaneously is an open question.

Enzyme-free autocatalytic systems, which are generally simpler than those with enzymes, are known to exponentially replicate one or a small set of species (1–5), but none of these systems replicate an arrangement of subunits defining a combinatorial sequence of information. Without the capacity for combinatorial information replication, open-ended evolution, in which complexity increases without bound (6), cannot occur.

Some RNA sequences have been shown to act as RNA polymerases that can assemble a general RNA sequence given a template (7). If such an RNA sequence polymerized a copy of itself, the required enzyme would be produced by the replication process, making it self-sustaining. However, fidelity sufficient for RNA-mediated RNA self-replication has not yet been observed (8, 9). Similarly, extension of nucleic acid primers can occur accurately without enzymes (10, 11), but it is not yet known whether

arbitrary sequences could be assembled this way; further difficulties are introduced by the need for the template and its newly assembled complement to separate before another round of replication can commence.

Homogeneous 2- and 3-dimensional crystal growth occurs spontaneously in nonliving systems and defect rates during crystal growth can be as low as error rates during genome replication (12). Like prion growth (13), crystal growth can be autocatalytic if mechanical forces fragment crystals, increasing the number of crystal growth fronts (14). If a crystal stored information in its arrangement of monomers, growth could propagate that information and scission could, by creating new growth fronts for propagation, replicate it. A crystal's information would then be subject to Darwinian evolution, as postulated by Cairns-Smith almost 50 years ago (15) (Fig. 1A). While replication of chemical sequences through crystal growth has continued to be of interest (16) because of its simplicity and potential compatibility with a wide variety of chemistries, such replication has never been demonstrated. The replication of information in the form of crystal defects has been observed, but fidelity was very low (17).

Here we show that DNA tile crystals (18, 19) can robustly replicate combinatorial information, as theoretically proposed earlier (20). DNA tiles are crystal monomers consisting of four to six synthetic strands of DNA folded into a double crossover structure (Fig. 1B). Tiles crystallize via sticky end hybridization (Fig. 1C), and under appropriate growth conditions, complementary sticky ends hybridize, while noncomplementary sticky ends are unlikely to interact.

We recently demonstrated that tiles can assemble ribbon-shaped crystals that propagate a sequence of information during growth (19). In that study, individual bits were copied highly accurately, but errors in propagation such as sequence truncation (i.e., the reduction of crystal width), or the spurious nucleation of crystals carrying new random sequences were more common. To decrease the rates of sequence truncation and spurious nucleation, we designed an improved tile set. The tiles in Fig. 1D form ribbons containing an arbitrary sequence of 2-tile-thick indigo (I) or orange (O) layers. During growth, only a tile matching the previous layer's color can attach favorably (i.e., sticky ends) (21, 22) (Fig. 1C and E), so ribbon growth propagates the sequence, one layer at a time (SI Appendix, Fig. S1). To improve fidelity, sequence copying is proofread: information is incorrectly propagated only if two tiles in a row misattach (23, 19). The gray

Author contributions: R.S., B.Y., and E.W. designed research; R.S. performed research; R.S. and B.Y. analyzed data; and R.S., B.Y., and E.W. wrote the paper.

The authors declare no conflict of interest.

This article is a PNAS Direct Submission.

Freely available online through the PNAS open access option.

<sup>1</sup>To whom correspondence should be addressed. E-mail: rschulm3@jhu.edu.

<sup>2</sup>Present address: Chemical and Biomolecular Engineering, Johns Hopkins University, Baltimore, MD 21218.

This article contains supporting information online at [www.pnas.org/lookup/suppl/doi:10.1073/pnas.1117813109/-DCSupplemental](http://www.pnas.org/lookup/suppl/doi:10.1073/pnas.1117813109/-DCSupplemental).

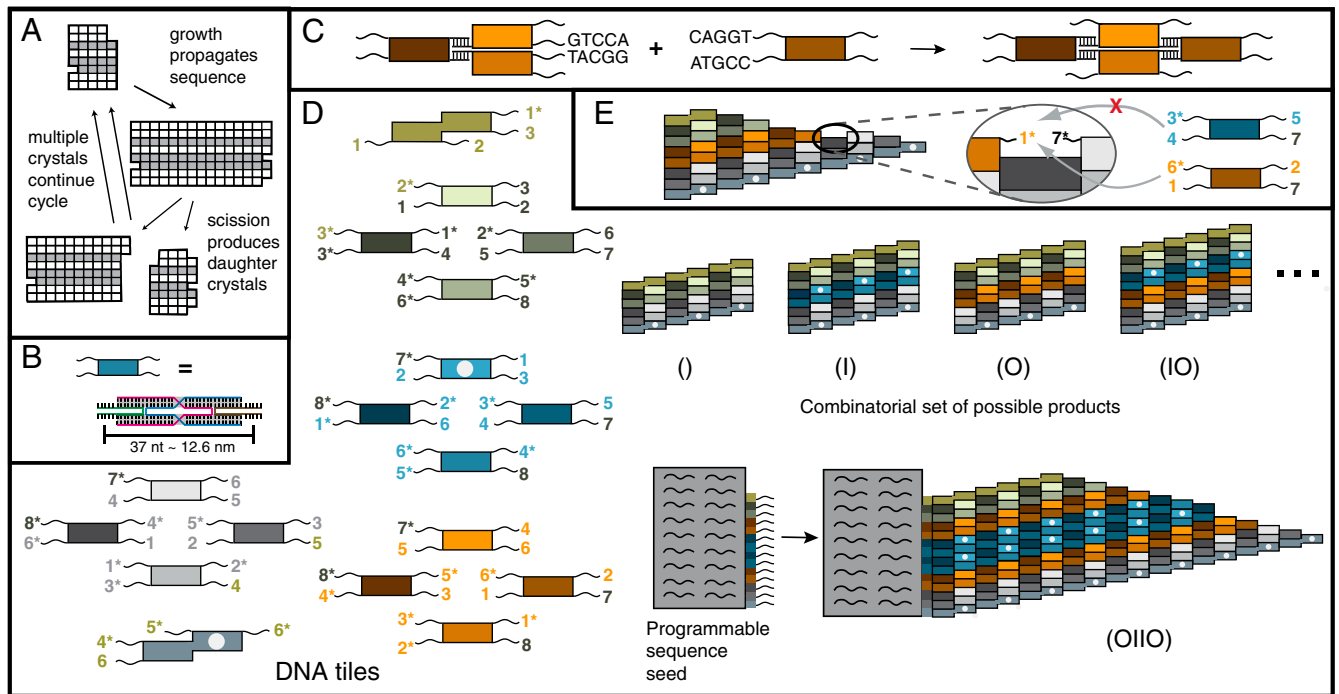


**Fig. 1.** Crystal replication. (A) An information sequence (here a column of white or black squares within a 2D crystal) is replicated in two stages. (B–E) DNA tile crystals. (B) DNA tiles are self-assembled, multihelical complexes with 5-nucleotide, single-stranded sticky ends. (C) Tiles attach to crystals via cooperative sticky end hybridization. (D) A tile set that can form ribbon crystals containing any sequence of indigo (I) or orange (O) tile blocks (or the null sequence). Using these tile types, an  $n$ -bit wide ribbon could carry any of  $2^n$  possible sequences. The two “double” tiles are edge tiles, while the four green tiles below the top edge tile and the four gray tiles above the bottom edge tile, create a thermodynamic barrier to the nucleation of new crystals (25, 24). The four indigo (blue) tiles are the I block tiles and the four orange tiles are the O block tiles. White dots are biotin; colored digits denote sticky end types. Sticky end complements have a \*. A crystal seed programmed with sticky ends for a sequence templates growth of that sequence. (E) To be favorable, tiles must attach by at least two sticky ends simultaneously, so growth copies the crystal sequence.

nucleation barrier blocks likewise make sequence truncation difficult by requiring that multiple tiles mismatch for truncation to occur. These tiles also increase the energetic barrier to new nucleation, making spurious nucleation of crystals not propagating the templated sequence rare (24, 25) (*SI Appendix, Supplemental Methods sections 1–3 and 12*).

## Results

**Crystal Growth.** To study whether DNA crystal sequences could be replicated via growth and scission, we characterized the increases in the numbers of crystal layers and growth fronts as we grew crystals (stage G1), created new growth fronts via scission (S1) and then continued growth (G2) (Fig. 2A). Without crystal seeds, tiles

produce an ensemble of crystal sequences dominated by those easiest to nucleate, crystals containing neither orange nor indigo layers (25, 24). To study the replication of a specific crystal sequence, we therefore programmed a DNA origami crystal seed (26, 19) to template crystals with the sequence OIOO (Fig. 1D and *SI Appendix, Fig. S2*). Previously, DNA crystals have been grown via annealing, which gradually increases tile interaction strength as temperature and concentration decrease. To permit cycles of growth and scission, we developed a method for constant temperature growth (*SI Appendix, Supplemental Methods sections 4 and 5*). To ensure consistently low supersaturation, tiles were not depleted during growth, and G1, S1, and G2 and transfers occurred in a temperature-controlled chamber. For G1, we mixed

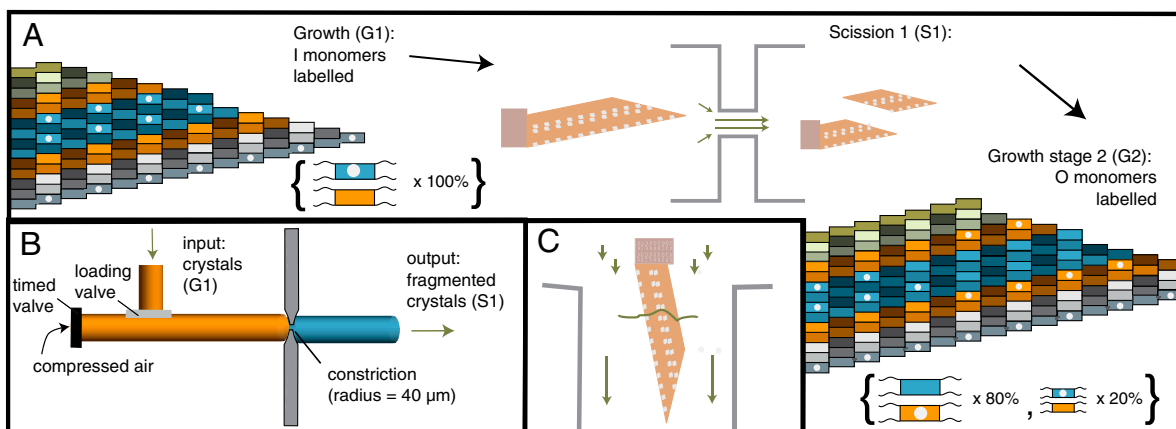


**Fig. 2.** Replication stages. (A) After growth (G1), crystals undergo scission (S1) and further growth (G2). (B–C) Scission mechanism. Compressed air propels solution containing crystals through a constriction (B), where high elongational flows fragment crystals [zoom, (C)]. Arrow lengths indicate rough fluid velocity.

**Continued Sequence Propagation.** To determine how well the new growth fronts could propagate their sequences, we diluted one part S1 mixture into four parts fresh monomers and let growth continue in the fresh mixture for 6–8 h (G2). In order to distinguish G2 growth from G1 growth, the fresh solution contained biotin-labeled O and unlabelled I tiles (Figs. 24 and 3).





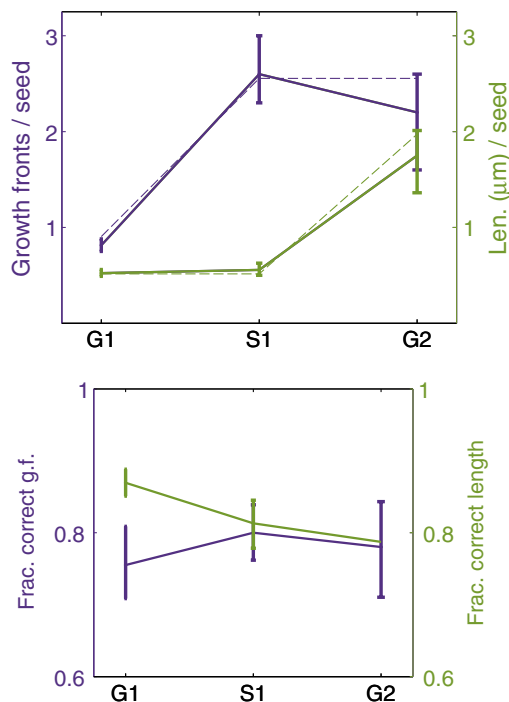


**Fig. 4.** Changes in the number and fraction of correct growth fronts and crystal length with replication stage. *Top:* Solid lines show measured number of growth fronts (purple) and crystal length (green) per seed. Dashed lines show the same values predicted by Eqs. 1–2 for the reported  $L_s[0]$ ,  $F_s[0]$  and the resulting best fits for  $f$  and  $g$ . *Bottom:* Fraction of correct growth fronts and fraction of crystal length that is correct, out of the total number of templated growth fronts and total templated crystal length, respectively. Errors here and elsewhere are 95% confidence intervals determined by bootstrapping.

After G2, there were  $1,750 \pm 400$  nm of correct layers per seed vs.  $620 \pm 40$  nm per seed after G1 (Fig. 4), suggesting that the new growth fronts increased the population's rate of sequence propagation; i.e., replication occurred. This increased rate of sequence propagation was observed despite the fact that around 20% of growth fronts appeared to be inactive; no layers were added to them during G2.

To determine the implied replication rate, we modified models of autocatalysis by simultaneous growth and stochastic scission (30, 31) to separate growth and scission into stages. For simplicity, the model does not consider mutation. For sequence  $s$ , the number  $F_s$  of growth fronts and the total length  $L_s$  of crystal layers after  $n + 1$  generations is

$$L_s[n+1] = L_s[n] + gF_s[n] \quad [1]$$

$$F_s[n+1] = F_s[n] + 2fL_s[n+1] \quad [2]$$

where  $g$  is the growth rate in nm per growth front per generation and  $f$  is the per nm probability of layer scission. Asymptotically,

$$F_s[n] = F_s[0]r^n,$$

and

$$L_s[n] = \frac{1}{2f} \left(1 - \frac{1}{r}\right) F_s[n],$$

with

$$r = 1 + fg + \sqrt{(1 + fg)^2 - 1};$$

i.e., growth is exponential with replication rate  $r$ . The best fit of our data to the model is  $f = 0.0016 \pm 0.0003$  and  $g = 570 \pm 90$ , for which  $r$ , the replication rate, is  $3.5 \pm 0.4$  (*SI Appendix, Supplemental Notes 6–8 and Fig. S14*). A replication rate of 3.5 implies that over many generations we would expect that the number of growth fronts and crystal layers bearing the OIIO sequence to increase by a factor of 3.5 per generation.

Sustained self-replication of a chemical sequence requires not only that the abundance of the sequence grow with each generation; mutants also must not replicate faster than the original sequence (27). In our experiments, mutants observably replicated (*SI Appendix, Fig. S15*), and in a few cases, crystals were twisted where G1 growth ended and G2 growth began incorrectly, suggesting crystal lattice defects (*SI Appendix, Fig. S16*). “Monster” crystals propagating >6 bits, which may have arisen via facet growth or side-to-side joining (*SI Appendix, Fig. S17*), and crystals joined end-to-end (*SI Appendix, Fig. S18* and Supplemental Note 9) were also observed during G2.

Surprisingly, however, almost the same proportion of templated growth fronts ( $78\% \pm 6$ ) and layers ( $79\% \pm 5$ ) were correct after G2 as after G1 (Fig. 4). The mutants also did not propagate faster than correct crystals: Between G1 and G2, the total number of incorrect growth fronts increased at the same rate as the number of correct growth fronts ( $3.2 \pm 0.5$  vs.  $3.1 \pm 1.0$ ). Similarly, incorrect and correct growth fronts added the same amount of length on average ( $530 \pm 290$  nm vs.  $460 \pm 140$  nm). To estimate whether the observed mutation rate and replication rate of mutants could allow sustained self-replication of the original OIO sequence, we simulated further generations using growth, scission and error rates sampled from the measured means and standard deviations. A simulated 1,000-fold replication of correct growth fronts took on average 7 generations, after which on average  $47\% \pm 35$  of templated crystals were correct (*SI Appendix, Supplemental Note 10*).

Like errors that change the sequence propagated during crystal growth or scission, spurious nucleation of crystals produces new mutants that can grow and replicate. Therefore, for sustained self-replication it is also necessary that spurious nucleation occur only rarely, so that spurious nuclei arise and replicate more slowly than crystals with the desired sequence. Spuriously nucleated crystals arose at  $1.7 \pm 0.6 \times 10^{-7}$  nM/s during G2 and  $0.9 \pm 0.3 \times 10^{-7}$  nM/s during G1 (*SI Appendix, Supplemental Notes 11 and 12*). After S1,  $14 \pm 7$  times more spurious growth fronts and  $19 \pm 9$  times more spurious layers were observed as after G1. However, almost all of these were observed after scission experiments where, unintentionally, the scission device audibly released cold air onto the crystals (*SI Appendix, Figs. S22 and S23*). Cool air increases supersaturation and could have temporarily increased spurious nucleation rates. When the 3 (of 6) experiments where cooling may have occurred are omitted (*SI Appendix, Fig. S22*), only  $0.6 \pm 0.4$  times as many spuriously nucleated layers and  $1.3 \pm 0.7$  times as many spuriously nucleated growth fronts were observed, respectively. Interestingly, the number of spuriously nucleated layers may have decreased because the forces applied to the crystals during scission could in some cases be enough to melt the spuriously nucleated crystals (*SI Appendix, Supplemental Note 13*). Therefore, these thinner crystals may have been selected against.

To determine how spurious nucleation would affect the replication process, we repeated the simulations of replication of the OIIO sequence, this time taking both mutation rates and spurious nucleation into account (an omitting the experiments where cooling may have occurred). We found that spuriously nucleated crystals would comprise only  $7\% \pm 14$  of crystals after 1,000-fold replication (*SI Appendix, Supplemental Note 10*). Thus this and the previous simulation support self-sustained, high-yield, 1,000-fold replication of the templated sequence (*SI Appendix, Fig. S24, Supplemental Note 14, and Tables S1–S2*).

PNAS | April 24, 2012 | vol. 109 | no. 17 | 6409

3. Rubinov B, Wagner N, Rapaport H, Ashkenasy G (2009) Self-replicating amphiphilic  $\beta$ -sheet peptides. *Angew Chem Int Ed* 48:6683–6686.
4. Lincoln TA, Joyce GF (2009) Self-sustained replication of an RNA enzyme. *Science* 323:1229–1232.
5. Carnall JMA, et al. (2010) Mechanosensitive self-replication driven by self-organization. *Science* 327:1502–1506.
6. Rasmussen S, et al. (2004) Transitions from nonliving to living matter. *Science* 303:963–965.
7. Johnston WK, Unrau PJ, Lawrence MS, Glasner ME, Bartel DP (2001) RNA-catalyzed RNA polymerization: Accurate and general RNA-templated primer extension. *Science* 292:1319–1325.
8. Wochner A, Attwater J, Coulson A, Holliger P (2011) Ribozyme-catalyzed transcription of an active ribozyme. *Science* 332:209–212.
9. Deck C, Jauker M, Richert C (2011) Efficient enzyme-free copying of all four nucleobases templated by immobilized RNA. *Nat Chem* 3:603–608.
10. Schrum JP, Ricardo A, Krishnamurthy M, Blain JC, Szostak JW (2009) Efficient and rapid template-directed nucleic acid copying using 2'-amino-2',3'-dideoxyribonucleoside-5'-phosphorimidazole monomers. *J Am Chem Soc* 131:14560–14570.
11. Kervio E, Hochges A, Steiner UE, Richert C (2010) Templating efficiency of naked DNA. *Proc Natl Acad Sci USA* 107:12074–12079.
12. Scheel HJ, Fukuda T (2003) *Crystal Growth Technology* (John Wiley and Sons).
13. Collins SR, Douglass A, Vale RD, Weissman JS (2004) Mechanism of prion propagation: Amyloid growth occurs by monomer addition. *PLoS Biol* 2:e321.
14. Viedma C (2005) Chiral symmetry breaking during crystallization: Complete chiral purity induced by nonlinear autocatalysis and recycling. *Phys Rev Lett* 94:065504.
15. Cairns-Smith AG (1966) The origin of life and the nature of the primitive gene. *J Theor Biol* 10:53–88.
16. Orgel LE, Crick FHC (1993) Anticipating an RNA world. Some past speculations on the origin of life: Where are they today? *FASEB J* 7:238–239.
17. Bullard T, Freudenthal J, Avagyan S, Kahr B (2007) Test of Cairns-Smith's crystals-as-genes hypothesis. *Faraday Discuss* 136:231–245.
18. Winfree E, Liu F, Wenzler LA, Seeman NC (1998) Design and self-assembly of two-dimensional DNA crystals. *Nature* 394:539–544.
19. Barish RD, Schulman R, Rothmund PWK, Winfree E (2009) An information-bearing seed for nucleating algorithmic self-assembly. *Proc Natl Acad Sci USA* 106:6054–6059.
20. Schulman R, Winfree E (2005) Self-replication and evolution of DNA crystals. *Advances in Artificial Life, 8th European Conference*, (Springer-Verlag, Berlin Heidelberg), Vol. 3630.
21. Mao C, LaBean TH, Reif JH, Seeman NC (2000) Logical computation using algorithmic self-assembly of DNA triple-crossover molecules. *Nature* 407:493–496.
22. Rothmund PWK, Papadakis N, Winfree E (2004) Algorithmic self-assembly of DNA Sierpinski triangles. *PLoS Biology* 2:e424–436.
23. Winfree E, Bekbolatov R (2004) Proofreading tile sets: Error-correction for algorithmic self-assembly. *DNA Computing 9*, eds J Chen and J Reif (Springer-Verlag, Berlin Heidelberg), Vol. LNCS 2943, pp 126–144.
24. Schulman R, Winfree E (2009) Programmable control of nucleation for algorithmic self-assembly. *SIAM J Comput* 39:1581–1616.
25. Schulman R, Winfree E (2007) Synthesis of crystals with a programmable kinetic barrier to nucleation. *Proc Natl Acad Sci USA* 104:15236–15241.
26. Rothmund PWK (2006) Folding DNA to create nanoscale shapes and patterns. *Nature* 440:297–302.
27. Eigen M, McCaskill J, Schuster P (1988) Molecular quasi-species. *J Phys Chem* 92:6881–6891.
28. Hariadi R, Yurke B (2010) Elongational-flow-induced scission of DNA nanotubes in laminar flow. *Phys Rev E* 82:046307.
29. Cloitre M, Mongruel A (1999) Dynamics of non-Brownian rodlike particles in a non-uniform elongational flow. *Phys Fluids* 11:773–777.
30. Schulman R, Winfree E (2008) How crystals that sense and respond to their environments could evolve. *Nat Comp* 7:219–237.
31. Knowles TPJ, et al. (2009) An analytical solution to the kinetics of breakable filament assembly. *Science* 326:1533–1537.
32. Seeman NC (2010) Nanomaterials based on DNA. *Ann Rev Biochem* 79:65–87.
33. Zhang DY, Yurke B (2006) A DNA superstructure-based replicator without product inhibition. *Natur Comp* 5:183–202.
34. Chandran H, Gopalkrishnan N, Yurke B, Reif J (2012) Meta-DNA: Synthetic biology via DNA nanostructures and hybridization reactions. *J R Soc Interface* rsif.2011.0819v1-rsif20110819.
35. Wang T, et al. (2011) Self-replication of information-bearing nanoscale patterns. *Nature* 478:225–228.
36. Fujibayashi K, Hariadi R, Park SH, Winfree E, Murata S (2008) Toward reliable algorithmic self-assembly of DNA tiles: a fixed-width cellular automaton pattern. *Nano Lett* 8:3554–3560.
37. Schulman R, Winfree E (2010) Simple evolution of complex crystal species. *DNA Computing 16*, eds Y Sakakibara and M Yongli (Springer-Verlag, Berlin Heidelberg), Vol. 6518.
38. Soloveichik D, Winfree E (2007) Complexity of self-assembled shapes. *SIAM J Comput* 36:1544–1569.
39. Winfree E (2006) Self-Healing Tile Sets. *Nanotechnology: Science and Computation*, eds J Chen, N Jonoska, and G Rozenberg (Springer-Verlag, Berlin Heidelberg), pp 55–78.
40. Chen HL, Goel A, Winfree E, Luhrs C (2007) Self-assembling tile systems that heal from small fragments. *Preliminary Proceedings of DNA Computing 13*, eds M Garzon and H Yan (Springer-Verlag, Berlin Heidelberg), Vol. LNCS 4848, pp 30–46.
41. Smalley RE, et al. (2006) Single wall carbon nanotube amplification: En route to a type-specific growth mechanism. *J Am Chem Soc* 128:15824–15829.
42. Li H, Carter JD, LaBean TH (2009) Nanofabrication by DNA self-assembly. *Mater Today* 12:24–32.
43. Wang H, Brandl DW, Nordlander P, Halas NJ (2007) Plasmonic nanostructures: Artificial molecules. *Acc Chem Res* 40:53–62.
44. Dutta PK, et al. (2011) DNA-directed artificial light-harvesting antenna. *J Am Chem Soc* 133:11985–11993.
45. Huppa JB, Davis MM (2003) T-cell-antigen recognition and the immunological synapse. *Nat Rev Immunol* 3:973–983.
46. Smith SB, Cui Y, Bustamante C (1996) Overstretching B-DNA: The elastic response of individual double-stranded and single-stranded molecules. *Science* 271:795–799.